Desalination and Water Treatment
www.deswater.com
doi: 10.1080/19443994.2015.1038592

57 (2016) 10616–10625
May

Taylor & Francis
Taylor & Francis Group

Evaluation of hydroxyl radical pathway and kinetic process for bubbling ozonation of methylene blue as reference compound

S. Zhang[a,b,*], D. Wang[c], P.P. Fan[a,b], L.P. Sun[a,b]

[a]*School of Environmental and Municipal Engineering, Tianjin Chengjian University, Jinjing Road 26, Tianjin 300384, China, Tel. +86 13820306663; Fax: +86 022 23085000; email: zssci1203@163.com (S. Zhang), Tel. +86 13820196660; email: 13820196660@163.com (P.P. Fan), Tel. +86 13920097721; email: slpyqs@vip.sina.com (L.P. Sun)*
[b]*Tianjin Key Laboratory of Aquatic Science and Technology, Tianjin 300384, China*
[c]*Key Laboratory of Industrial Ecology and Environmental Engineering (MOE), School of Environmental Science and Technology, Dalian University of Technology, Linggong Road 2, Dalian 116024, China, Tel. +86 13940950507; email: wangdong@dlut.edu.cn*

Received 9 October 2014; Accepted 29 March 2015

ABSTRACT

Ozonation experiments were conducted in a bubble column reactor taking methylene blue (MB) as model compound, where the role of solution pH and organic load as basic parameters of wastewater influencing pathway of hydroxyl radical ($HO^{\bullet}$) and the kinetics were investigated. The relative significance of $HO^{\bullet}$-pathway was evaluated compared to molecular ozone in both kinetics and degradation process. Results showed that, as solution pH increased from 5 to 11, the contribution of $HO^{\bullet}$ (labeled as θ) got intensified from 0.05 up to 0.80 (apparent $HO^{\bullet}$ abundance proliferated up to 35.76×10^{-7} M), giving rise to an exponential growth of pseudo-first-order rate constant as well as an enhanced mineralization. Reduction of initial organic concentration ($[C]_{0,MB}$) retarded chemical gas-to-liquid absorption of ozone and the global degradation of MB, while interestingly at the same time, the kinetic rate constant on MB decolorization accordingly began to grow up since the $HO^{\bullet}$-pathway impact substantially got reinforced (θ elevated from 0.80 up to 1.944 when $[C]_{0,MB}$ decreased from 80 to 20 mg L^{-1} under pH 11).

Keywords: Ozonation; Bubble column; Hydroxyl radical; Kinetic process; Degradation

1. Introduction

Bubbling ozone treatment (BOT) has received increasing application over the last decade as an alternative quick-response treatment strategy dealing with contaminated waters [1–5]. It commonly took place in column reactors with operational simplicity, where bubbling introduction of ozone can induce a complete back-mixing in favor of contact reaction and mass transfer between phases, allowing BOT to accomplish oxidative abatement of color and organic substances in one step without generation of sludge or solid wastes. Two concurrent pathways principally account for the process of BOT, i.e. oxidation by molecular ozone (O_3) as well as by hydroxyl radical ($HO^{\bullet}$) generated from hydrolysis of ozone. Direct O_3 attack is relatively weak due to the selectivity and low power ($E^0(O_3/H_2O) = +2.07$ V) as only aromatic compounds with nucleophilic positions or unsaturated aliphatics may be effectively degraded [6], while the $HO^{\bullet}$, with highly electron-withdrawing

*Corresponding author.

nature ($E^0(HO^{\bullet}/H_2O)$ = +2.80 V), can lead to an outcome of advanced oxidation that is more responsible for improvement of organoleptic properties such as taste and color, disruption of bio-toxic or persistent organic pollutants, and oxidative removal of total organic carbon (TOC) [7]. Thus, BOT can be recommended as a feasible and promising technology for remediation of wastewaters in environmental engineering, for which the intensification of $HO^{\bullet}$-pathway and kinetic process control are regarded of practical significance.

Basic solution environment has been proved to be favorable for development of $HO^{\bullet}$-pathway during ozonation, which can enlarge the intervention of $HO^{\bullet}$ populations for deep oxidation and even disruption of extreme persistent organic pollutants as perfluorooctane sulfonate [8]. This is because the presence of hydroxide ion (OH^-) can act as effective initiator for transformation of aqueous ozone into $HO^{\bullet}$ radicals referring to Staehelin and Hoigné [9], and following chain steps of ozonolysis, the elevation of solution pH will readily enhance the production of $HO^{\bullet}$ species. In progress of BOT moreover, ozone molecules penetrate from gas phase into the liquid giving rise to an accumulation of aqueous O_3, and in the meantime, associated bulk reactions depleting the transferred O_3 will readily take place. On this regard, the kinetics of BOT should be dictated by the coupling effect of gas-to-liquid ozone transfer and consumption of aqueous O_3, and the latter includes mainly the O_3 hydrolysis yielding of $HO^{\bullet}$ (mainly affected by solution pH) as well as the reduction by organic pollutants. For a designated operational flow regime associated with volumetric ozone transfer coefficient [10], therefore, kinetics of ozonation treatment in column reactor should not only depend on solution pH, but be stoichiometrically subject to the concentration of reductive organic matter that coupled to total molecular activity. The global impact of pH or the organic load on kinetic rate constant of ozonation has been presented in some literatures [11–13], while in application of BOT technology involving the process of ozone penetration, accumulation, transformation, and consumption, more information should be extracted to evaluate the significance of $HO^{\bullet}$-pathway and the kinetics for a better process control.

In this work, we performed ozonation of methylene blue (MB) in a bubble column reactor taking solution pH and organic concentration as influential factors, where the intervention of $HO^{\bullet}$ in contribution to the degradation of MB was analyzed and the overall kinetic process was evaluated. Here, MB was chosen as model organic contaminant, since it is widely used for dyeing cotton and wool as colored synthetic chemical [14], and it has extensive pharmacological utilization as phenothiazine derivative with antibiotic nature [15].

2. Experimental

2.1. Ozonation procedure

Ozonation experiments were conducted in a semi-batch bubble column reactor (inner diameter × height = 0.1 m × 1.8 m) as illustrated in Fig. 1. Compressed air undergoing drying/filtration was controlled to pass through an ozonizer (O_3 yield of 100 g h^{-1}), and then, the mixed gaseous ozone (containing mainly O_3, O_2, and N_2) was bubbling-introduced into the column reactor through a perforated plate. Superficial gas velocity performed to dominate the flow pattern in the manner of homogeneous, transition, and heterogeneous regimes similar to that reported by Krishna et al. [16] (see inset of Fig. 1), and for this work, all ozonation experiments were controlled to take place in heterogeneous regime with gas flow rate of 3.25 m^3 h^{-1} for a complete backmixing and intense gas-to-liquid ozone transfer. Preset amount of methylene blue ($C_{16}H_{18}ClN_3S{\cdot}3H_2O$, analytical grade) was employed as the organic solute and dissolved without further purification in 8 L ultrapure water as the liquid phase for ozone treatment tests. The pH was initially adjusted by adding 0.1 M HCl or 0.1 M NaOH solutions and maintained during reactions by means of dropwise regulation. All the experiments were conducted under ambient temperature (23–25°C) and atmospheric pressure.

2.2. Analysis methods

Concentration of $HO^{\bullet}$ was measured by the coumarin fluorescence probing technique as described by Maezono et al. [17] since coumarin molecule is capable to trap $HO^{\bullet}$ radical generating luminescent 7-hydroxycoumarin. The fluorescent emission spectra were measured for various concentration of 7-hydroxycoumarin from 10^{-7} to 6×10^{-6} M, and as the calibration curve for determination of apparent $HO^{\bullet}$ concentration, the fluorescence intensity at the wavelength of 470.4 nm linearly grew up with increasing 7-hydroxycoumarin concentration (see the supplementary figure).

MB concentration was measured using 756PC UV/Vis spectrometer at wavelength of 664 nm according to Lambert–Beer's law. TOC was determined by TOC-VCPH analyzer (Shimadzu, Japan). Solution pH was detected by a digital pH meter (Cyber Scan pH 1500). Ozone concentrations in respective gas and

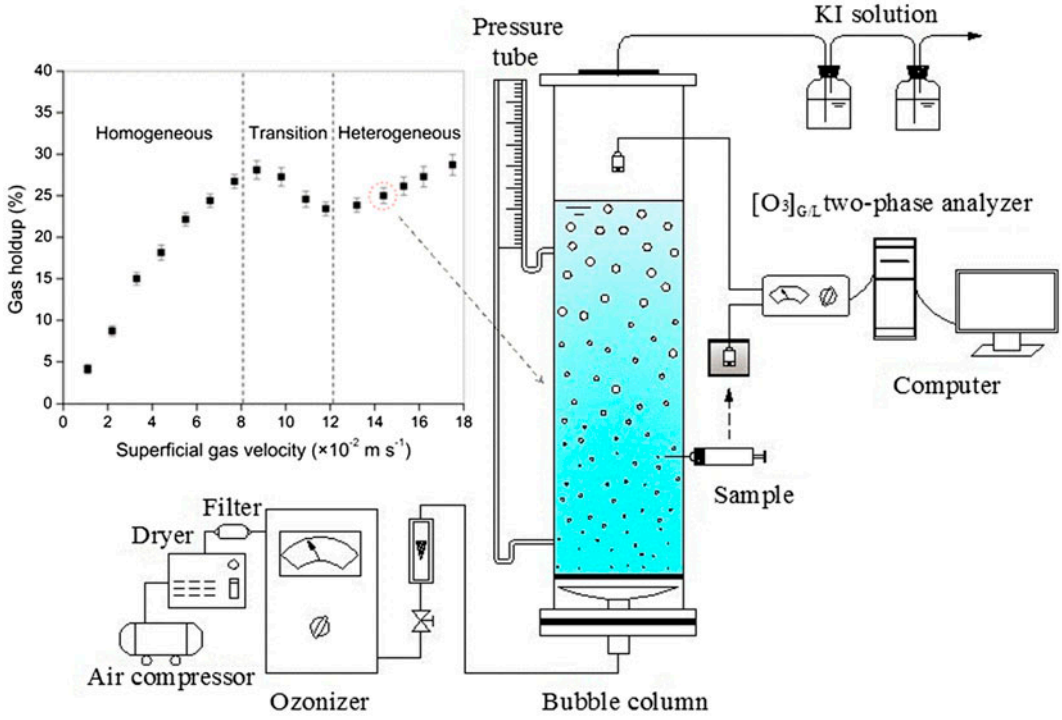

Fig. 1. Schematic diagram of experimental setup (Inserted figure: Evolution of gas holdup as a function of superficial gas velocity; error bars represent the standard deviation of duplicate experiments).

liquid phases were monitored by Portable-BD5Gas2610 Ozone Analyzer (BigDipper Co. Ltd, Beijing, China).

Gas holdup (ε_g) was determined based on the difference of liquid heights in the two pressure tubes during bubbling reaction and can be simplified as expressed by Eq. (1),

$$\varepsilon_g = \frac{\Delta h}{H} \times 100\% \quad (1)$$

where Δh is the liquid heights discrepancy of the two pressure tubes during bubbling process, and H represents the vertical distance of the two points alongside column wall for fix of pressure tubes (0.7 m for this work).

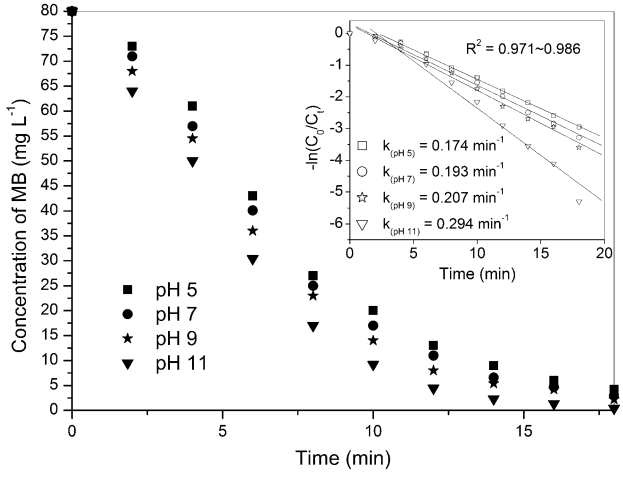

Fig. 2. Decolorization of MB at initial concentration of 80 mg L^{-1} during ozonation under solution pH of 5, 7, 9, and 11, respectively (Inserted figure: Linear fit for MB decolorization kinetics during ozonation).

3. Results and discussion

3.1. Effect of solution pH

Fig. 2 shows the profile of MB disappearance during ozonation as a function of solution pH adjusted in the range of 5–11, where the discoloration process following pseudo-first-order kinetics (see inserted figure) generally presented to be accelerated as the solution alkalinity gradually increased. In most cases, ozonation processes occur mainly through a combination of the molecular ozone (O_3) and hydroxyl free radical ($HO^{\bullet}$) pathways, and correspondingly, the oxidation kinetics of MB could be established by Eq. (2),

$$-\frac{d[C]}{dt} = k_{O_3}[C][O_3]_L + k_{HO\cdot}[C][HO^{\cdot}] \quad (2)$$

where [C] is the MB concentration, t is the reaction time, k_{O_3} and $k_{HO\cdot}$ are the second-order rate constants, and $[O_3]_L$ and [HO•] are the respective concentration of aqueous ozone and hydroxyl radical.

Elevation of solution pH means a significant concentration of hydroxyl anions (OH^-) that has been concluded as an effective "initiator" for decomposition of dissolved ozone yielding HO• species [9], and the intervention of highly oxidative HO• populations will lead to a much stronger disruption of most organic substances including also the breakage of MB as noticed in this study. In contrast, Soares et al. [12] documented a negative impact of pH adjusted up to 11 on kinetics of color removal dealing with an acid dye (Acid Blue 113), which is quite different to the outcome of this work. This could be explained by the fact that the chromophore groups of Acid Blue 113 as model compound are much easier to be destructed by molecular ozone (O_3), while basic pH would incur significant conversion of O_3 into HO• that had impaired largely the availability of O_3 (transferred from gas to liquid) being more selective for decolorization of the target molecule. Referring to the pH effect obtained in this study, the degradation of MB can therefore be attributed to both direct O_3 attack and the oxidation of HO• radicals as expressed in kinetic form by Eq. (2), and the HO• exhibited higher effectiveness through electrophilic attack by cleavage of the conjugated chromophores in MB molecules than the nucleophilic attack by O_3. The above comparison suggested that the significance of HO• species and its pathway contribution to kinetics are in association with the "sensitivity" of target contaminant in response to O_3 and HO• attack, which should be analyzed prior to a rational adjustment on the acid–base property of wastewaters.

Basic solution environment in favor of ozone treatment has been indicated in literature using overall rate constant as a reflection of intensification in HO•-induced advanced oxidation such as dealing with atenolol [18]. To gain an insight, we tried to establish a quantitative description of pH impact on the contribution of HO•-pathway to ozonation kinetics. The process of ozone hydrolysis for generation of HO• follows sequential steps delineated by Reactions (3)–(7) referring to research works by Staehelin and Hoigné [9] as well as Bűhler et al. [19],

$$O_3 + OH^- \xrightarrow{k_1} HO_2^- + O_2 \quad k_1 \approx 70\ M^{-1}\ s^{-1} \quad (3)$$

$$O_3 + HO_2^- \xrightarrow{k_2} HO^{\cdot} + {}^{\cdot}O_2^- + O_2 \quad k_2 \approx 2.8 \times 10^6\ M^{-1}\ s^{-1} \quad (4)$$

$$O_3 + {}^{\cdot}O_2^- \xrightarrow{k_3} {}^{\cdot}O_3^- + O_2 \quad k_3 \approx 1 \times 10^9\ M^{-1}\ s^{-1} \quad (5)$$

$${}^{\cdot}O_3^- + H_2O \xrightarrow{k_4} HO_3^{\cdot} + OH^- \quad k_4 \approx 5.2 \times 10^{10}\ M^{-1}\ s^{-1} \quad (6)$$

$$HO_3^{\cdot} \xrightarrow{k_5} HO^{\cdot} + O_2^{\cdot} \quad k_5 \approx 1.1 \times 10^5\ M^{-1}\ s^{-1} \quad (7)$$

In light of the above chain reactions taking place in time sequence, it is clear that Reaction (3), with rate constant (about $70\ M^{-1}\ s^{-1}$) at least five order of magnitude lower than the others, should act as the limiting step for ozonolysis producing HO•. Assuming a very fast depletion of HO• by MB molecules in a fraction exponentially related to the population of HO• once created (labeled as γ), the second term on right hand of Eq. (2) could be expressed by Eq. (8) as a function indicating the decay rate of MB by HO•-pathway, taking into consideration that each three molar O_3 coupled stoichiometrically to a yield of two molar HO• based on Reactions (3)–(7).

$$k_{HO\cdot}[C][HO^{\cdot}] = \left(\frac{3[O_3]_L[OH^-]k_{HOO^-}}{2}\right)^{\gamma} \quad (8)$$

where $[OH^-]$ represents the concentration of hydroxyl anions and k_{HOO^-} is the second-order rate constant for formation of hydrogen peroxide anion as the initiative step indicated by Reaction (3).

Eq. (8) reflects the fact that pH enhancement with greater amount of HO^- will induce an enlargement of HO• population by expediting decomposition of aqueous ozone, and the subsequent fast depletion of HO• by MB molecules could in theory exhibit positive correlation with $[OH^-]$ as well as a sufficient provision of dissolved O_3 transferred from ozone-spiked bubbles. Hence, we may substitute Eq. (8) into Eq. (2) yielding Eq. (9),

$$-\frac{d[C]}{dt} = k_{O_3}[C][O_3]_L + \left(\frac{3[O_3]_L[OH^-]k_{HOO^-}}{2}\right)^{\gamma} \quad (9)$$

Considering the decolorization kinetics conformed pseudo-first-order process, the bulk concentration of

O_3 (i.e. $[O_3]_L$) should perform in a steady state manner as a consequence of ozone feeding and consumption, and it is indeed the case as was detected during experiments (discussed in Section 3.2). Taking the value of MB concentration as ozonation commenced (labeled as $[C]_{0,MB}$), Eq. (9) can be simplified as Eq. (10),

$$k = \alpha + \beta[OH^-]^{\gamma} \tag{10}$$

where k denotes the overall rate constant determined from experimental data and constants α and β represent the respective terms of $k_{O_3}[O_3]_L$ and $\left(\frac{3[O_3]_L k_{HOO^-}}{2}\right)^{\gamma} \cdot \frac{1}{[C]_{0,MB}}$ in Eq. (9).

As a consequence, α, β, and γ can be computed using multiple non-linear regression analysis (0.162, 0.513, and 0.199 respective for α, β, and γ with R^2 of 0.981), and results calculated concerning the evolution of rate constant (k) as a function of solution pH can be exhibited in the form of Eq. (11).

$$k \approx 0.162 + 0.513 \times 10^{\left(\frac{pH}{5} - 2.8\right)} \quad (R^2 = 0.981) \tag{11}$$

Correspondingly, the contribution (labeled as θ) of HO•-pathway compared to O_3 attack for oxidative destruction of MB can be determined as shown in Fig. 3, which is defined as the numerical ratio of the second term to the first term in the right hand of Eq. (9).

Referring to the results of Eq. (10) obtained by non-linear regression analysis where the value of α (i.e. $k_{O_3}[O_3]_L$) was determined to be 0.162 min^{-1} (equivalent to 2.7×10^{-3} s^{-1}), the parameter k_{O_3} can then be calculated through dividing α by the concentration of aqueous O_3 (i.e. $[O_3]_L$) during ozonation. Noting that the average apparent concentration of O_3 during reactions was in a rather low level (about 36 μg L^{-1} for $[C]_{0,MB}$ of 80 mg L^{-1}), we hereby can get the approximate k_{O_3} value of 3.6×10^3 M^{-1} s^{-1} which is higher than many organic substances but in a similar level as that of glyphosate being a broad-spectrum herbicide [20]. Hydroxyl radical (HO•), as a key oxidant accounting for ozonation, is extremely powerful whose rate constants with organic molecules are generally in the range of 10^8–10^{10} M^{-1} s^{-1} [21]. One can see from Fig. 3 that the contribution of HO•-pathway to ozonation kinetics of MB was clearly weaker than that completed by O_3 for pH scenarios around or lower than nine, whereas when the solution basicity intensified to pH 11, the θ substantially increased and reached a level up to 0.8, indicating the HO•-effect on MB discoloration kinetics was then almost comparable to aqueous O_3.

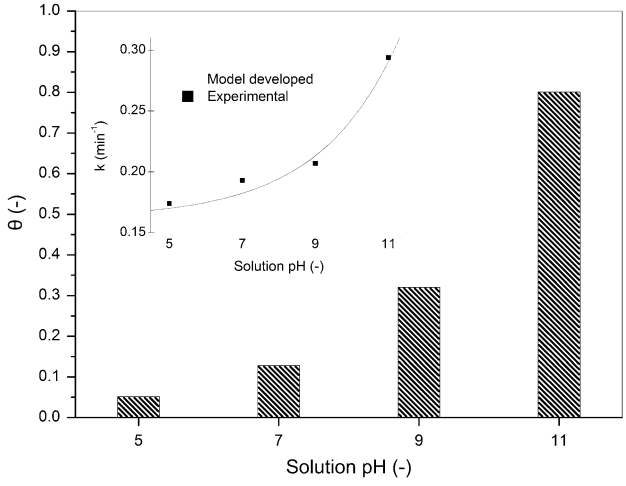

Fig. 3. Contribution ratio (θ) of HO• to aqueous O_3 for decolorization kinetics of MB during ozonation (Inserted figure: Evolution of pseudo-first-order rate constant as a function of solution pH).

The outcome of θ is just a reflection of HO•-pathway influence on ozonation of a target organic molecule (MB for this work), but can hardly represent all the roles played by HO• such as the mineralization by advanced oxidation. This is because the intervention of HO• oxidant, only a fraction of which was captured by MB, will give rise to a simultaneous deep oxidation of the daughter products and their intermediate fragments from the parent molecule (i.e. MB), resulting in a mineralization effect being an important issue for ozone science. Nevertheless, the non-selective nature of HO• makes it to be vulnerable and short-lived species that can even rapidly interact with inorganic substances such as carbonate or bicarbonate ions as terminative production. Then, the stoichiometry of HO• population should be regarded as a key controlling factor for the occurrence of mineralization process. To gain more straightforward evidence, we comparatively followed up the evolution of apparent HO• concentrations over time under different pH cases during ozonation and results are shown in Fig. 4. The abundance of HO• as expected got enlarged as solution basicity enhanced, which was particularly pronounced as pH increased from 9 to 11 with the corresponding HO• concentration proliferated from 11.52×10^{-7} M to 35.76×10^{-7} M, and the latter was about 18.4 times amount of that detected at pH 5 (1.94×10^{-7} M) and 9.2 times of that detected at pH 7 (3.90×10^{-7} M). Consequently, the TOC was remarkably removed (close to 80%) at pH 11 in the progress of ozonation over 180 min, while it cannot be abated even to a half amount for other cases tested within the same time period.

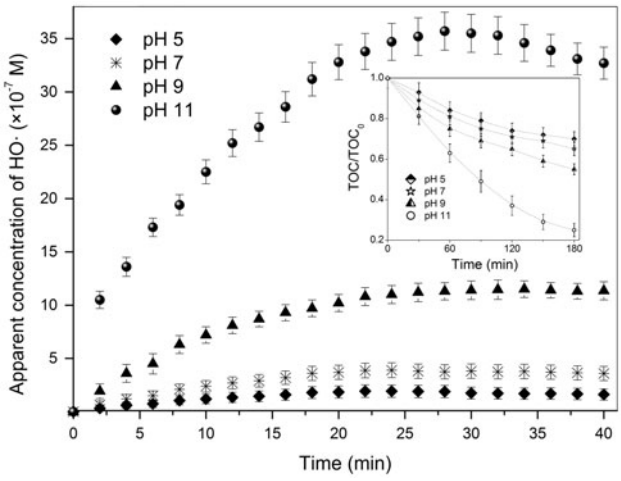

Fig. 4. Profile of apparent concentration of hydroxyl radicals (HO•) during ozonation of MB under solution pH of 5, 7, 9, and 11, respectively (Inserted figure: Evolution of dimensionless TOC during ozonation of MB; error bars represent the standard deviation of duplicate experiments).

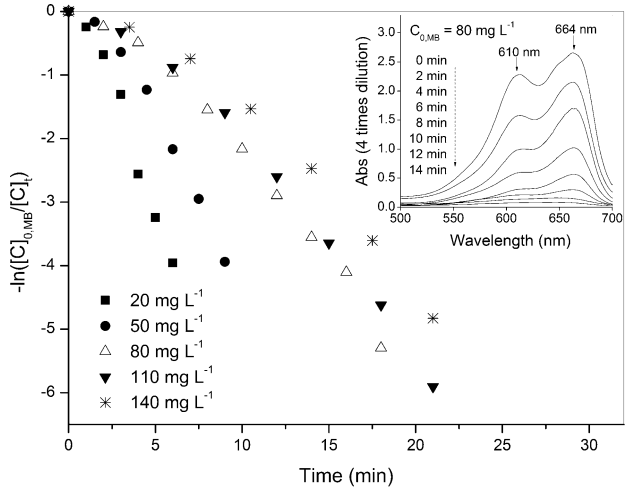

Fig. 5. Decolorization kinetics at pH 11 during ozonation with initial MB concentrations ($[C]_{0,MB}$) of 20, 50, 80, 110, and 140 mg L^{-1}, respectively (Inserted figure: The UV/vis absorption spectra of 4-times-diluted liquid samples withdrawn at time interval of 2 min under $[C]_{0,MB}$ of 80 mg L^{-1}).

3.2. Effect of organic concentration

It was demonstrated that ozonation of MB as model aromatic compound is completed both by molecular ozone (O_3) and hydroxyl radical (HO•), and the oxidation kinetics performed to subject to solution pH controlling the intensity of HO•-pathway. For a preset pH level, however, the coefficient θ is not an absolute constant for all ozonation cases since it is subject to the nature of contaminant species as aforementioned and may also be influenced by the concentration of target organics coupled to the chemical activity. As shown in Fig. 5, ozonation efficiency got substantially accelerated as initial concentration of MB decreased, and the inset figure shows a rapid drop in absorbance at 664 nm designating the disappearance of MB (610 nm for dimmer of MB molecules). Meanwhile, the rise of aqueous O_3 was clearly fettered by the presence of MB causing $[O_3]_L$ levels to remain low in time period for decolorization (see Fig. 6), and the superficial concentration

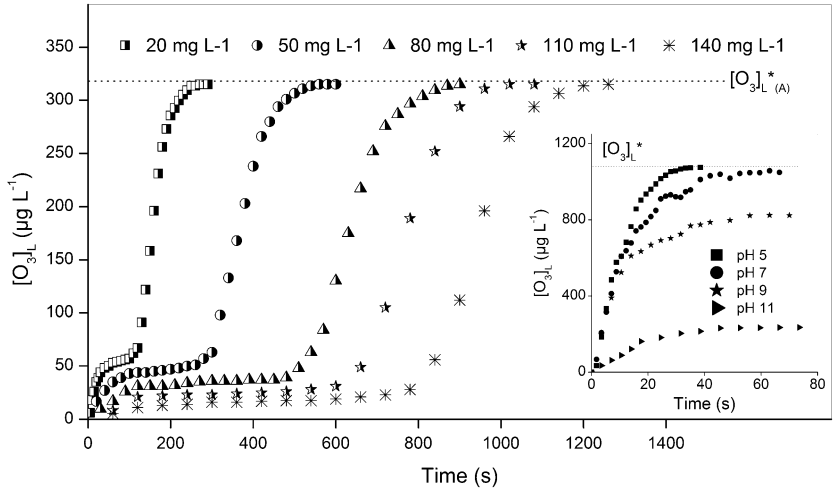

Fig. 6. Concentration profile of aqueous ozone ($[O_3]_L$) over time during ozonation of MB with $[C]_{0,MB}$ of 20, 50, 80, 110, and 140 mg L^{-1}, respectively (Inserted figure: Bubbling-induced evolution of $[O_3]_L$ over time in pure water under solution pH of 5, 7, 9, and 11, respectively).

of O_3 discriminated among the cases with different initial MB concentrations. The average values of aqueous O_3 concentrations as a function of initial MB load are listed in Table 1, among which the $[C]_{0,\,MB}$ of 20 mg L^{-1} resulted in a relative higher $[O_3]_L$ compared to others, and the $[O_3]_L$ tended to drop down with increasing $[C]_{0,\,MB}$ level (also can be seen in Fig. 6). As a consequence of higher O_3 concentration, the overall rate constant (see Table 1) increased in response to the decreasing $[C]_{0,\,MB}$, following the chemometrics as expressed by Eq. (9).

To the opposite, Lackey et al. [22] in ozonation of Acid Yellow 17 reported that the rate constant decreased over time as target compound gradually eliminated from 100 to 1 mg L^{-1}, and they attributed this phenomenon to an enhanced demand for aqueous ozone. Actually, the accumulation of aqueous O_3 largely depends on the rate of gas–liquid ozone transfer prior to the depletion by bulk reactions, and mass transfer between phases is controlled by both the driven force subject to saturated O_3 concentration (labeled as $[O_3]_L^*$ in the inset of Fig. 6) as well as the hydrodynamics affecting the volumetric gas–liquid mass transfer coefficient [10]. For Lackey et al. [22] the introduction of ozone was 79.20 mg min^{-1} at gas flow rate of 3.78 L min^{-1}, resulting in the concentration of gaseous O_3 at about 20.95 mg L^{-1}, while in this work, the actual concentration of gaseous ozone produced by ozonizer was detected at about 65 mg L^{-1}, indicating a more than three times higher of driven force at the beginning of ozonation. Moreover, the hydrodynamics during bubbling ozonation was controlled in heterogeneous flow regime with superficial gas velocity of 0.144 m s^{-1} (see Fig. 1), which means a complete mixing state benefiting the gas-to-liquid ozone transfer. For this study, therefore, the concentration of aqueous O_3 can be maintained in a relatively steady state in process of reactions consuming ozone in an extreme fast velocity, thus guaranteed an adequate supply of ozone and in turn gave rise to pseudo-first-order kinetic profiles as analyzed. Thus, gas-to-liquid ozone transfer should be taken into consideration for evaluation of kinetics in bubbling ozonation processes.

As ozonation progressed to the time point for a significant disappearance of MB (to about 6 mg L^{-1}), the $[O_3]_L$ suddenly began to grow up until it attained a steady state as shown in Fig. 6, which should be assigned to the counteraction of O_3 transferred from gas to liquid with that depleted in the bulk phase mainly by OH^-. The inset of Fig. 6 exhibits the evolution of $[O_3]_L$ in pure water (no MB present) as a function of consecutive bubbling of ozone at solution pH of 5, 7, 9, and 11, respectively. It can be seen for basic pH of 11 that the $[O_3]_L$ remained largely depressed even in scenario free from MB, indicating the fast depletion of O_3 molecules by OH^- following mainly Reaction (3) that overshadowed the accumulation of O_3 by gas–liquid mass transfer. However, the "screening effect" of solution pH on gas–liquid mass transfer of O_3 was seemingly remain weaker compared to the consumption of O_3 in reaction with MB, since transitional time points of $[O_3]_L$ exhibited to be subject to the concentration of MB, and correspondingly the process of ozone transfer between phases got concealed particularly in time period for MB discoloration. This phenomenon is because the presence of MB will simultaneously result in a direct chemical absorption of aqueous O_3 as well as a fast depletion of $HO^{\bullet}$, and the latter behavior will additionally accelerate the consumption of dissolved ozone. Turning to parameter θ as the relative contribution of $HO^{\bullet}$ to O_3 according to Eq. (9), the impact of $HO^{\bullet}$-pathway dealing with MB under basic solution (pH 11 adopted) has an inverse correlation with the concentration of both aqueous O_3 and target molecule (i.e. MB) as can be expressed by Eq. (12).

$$\theta \propto \frac{1}{[C][O_3]_L^{1-\gamma}} \tag{12}$$

For determination of θ, we could substitute the MB concentration as ozonation launched (i.e. $[C]_{0,MB}$) for [C] term, replace $[O_3]_L$ by average concentration of aqueous O_3 during decolorization period (labeled as $\overline{[O_3]_L}$), and take the value of γ as 0.199 computed by

Table 1
Parameters relevant to ozonation of MB at pH 11

$[C]_{0,MB}$ (mg L^{-1})	$\overline{[O_3]_L}$ (μg L^{-1})	k (min^{-1})	R^2 (−)	θ (−)	$\frac{d[C]_{0,MB}}{dt}$ (mg (L min)$^{-1}$)
20	67.4	0.705	0.966	1.944	14.10
50	48.2	0.445	0.962	1.017	22.25
80	36.1	0.294	0.971	0.801	23.52
110	24.4	0.286	0.973	0.797	31.46
140	18.1	0.234	0.957	0.795	32.76

multiple non-linear regression analysis based on Eq. (10). Results shown in Table 1 revealed that the contribution of HO· exhibited to be influenced not only by solution pH as discussed in Section 3.1, but by the abundance of MB as model organic reactant. Interestingly, the reduction of $[C]_{0,MB}$ allowed an enlarged contribution of HO· oxidant referring to θ, which was especially evident for $[C]_{0,MB}$ of 20 mg L^{-1} with θ growing up to 1.944. A proper explanation may be that the apparent concentration of O_3 can be maintained in a relative high level because of lowered MB concentration, which could be captured more easily by OH^- under basic environment (pH 11) to generate HO· following Reactions (3)–(7). Then, the abundance of HO· populations got extended and the HO·-pathway for advanced oxidation was intensified eventually.

It should be underlined that elevation of overall rate constant associated with decreasing $[C]_{0,MB}$ is just a reflection of kinetic process, while it did not link to a faster disappearance in the molar amount of MB and its by-products (i.e. the total ozonation efficiency for degradation of MB). Based on pseudo-first-order kinetic result, Eq. (2) can be transformed into a global format as shown in Eq. (13),

$$\frac{d[C]}{dt} = k[C] \tag{13}$$

where k denotes the overall rate constant for ozonation of MB.

The disappearance of MB per unit time $\left(\text{namely the term } \frac{d[C]}{dt}\right)$ was subject to both the kinetic rate constant and the concentration of target contaminant. Referring to Table 1, the total disruption rate of MB once ozonation commenced $\left(\text{namely the term } \frac{d[C]_{0,MB}}{dt}\right)$, opposite to the trend of k, grew up with an increasing initial amount of MB, indicating an intensified chemical absorption of ozone.

The chemical consumption of gaseous ozone was defined by Eq. (14) for which the relevant parameters were online monitored.

$$\text{Ozone consumption } (\%) = \frac{[O_3]_{G,in} - [O_3]_{G,out}}{[O_3]_{G,in}} \times 100\% \tag{14}$$

where $[O_3]_{G,in}$ and $[O_3]_{G,out}$ represent the inlet and outlet of gaseous ozone concentration, respectively.

Results are illustrated in Fig. 7. One can see that the bubbling system with higher MB load allowed more vigorous absorption of ozone compared to that with lower MB amount (particularly evident as $[C]_{0,MB}$ dropped to 20 mg L^{-1} or totally absent), which is indicative of an efficient utilization of gaseous O_3 once entered the liquid bulk where MB was highly concentrated. The result is also indicative that the driven force accounting for gas-to-liquid ozone transfer (i.e. $[O_3]^*_L - [O_3]_L$) should be in a relative higher state with increasing MB concentration. And this inference was in accordance with the fact that the rise of aqueous O_3 was substantially suppressed in the progress of ozonation especially for scenarios where more MB concentrated (see Fig. 6).

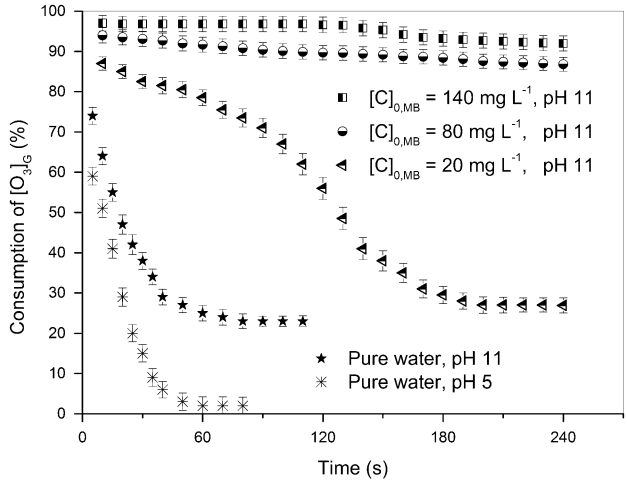

Fig. 7. Consumption rate of gaseous ozone ($[O_3]_G$) over time in bubbling ozone systems with and without MB solute (Error bars represent the standard deviation of duplicate experiments).

4. Conclusions

Basic pH environment for ozonation processes is known to benefit the generation of HO· inducing advanced oxidation through chain steps of O_3 hydrolysis (more likely by Reactions (3)–(7)), while besides this set of decomposition behavior yielding HO·, aqueous O_3 being transferred from gas phase (bubbles) to liquid bulk should simultaneously be consumed by the presence of reductive organic substances (such as MB employed in this work). Then the kinetic process by ozonation should be dictated by some fundamental controlling factors including solution pH, concentration of organic contaminant, and feeding of aqueous O_3 by gas-to-liquid mass transfer, and their implications during ozonation require further discussion/evaluation by laboratory works in order to gain an insight for a better process control.

In this work, kinetic study was conducted in a bubbling ozone reactor dealing with methylene blue (MB) as model compound, where the effects of solution pH and organic load (i.e. MB concentration) were investigated. Reaction experiments were operated in heterogeneous flow regime allowing a complete back-mixing and sufficient gas–liquid ozone transfer. To make quantitative evaluation for the impact of hydroxyl radical ($HO^{\bullet}$) pathway on kinetic process, we established and analyzed parameter θ that was designated to the contributive ratio of $HO^{\bullet}$ on degradation of MB compared with direct O_3 attack. Results demonstrated that elevating solution pH or interestingly lowering organic abundance would induce a substantial intensification of $HO^{\bullet}$-pathway (i.e. enhancement of θ) and an increment of kinetic rate constant for decolorization of MB as target contaminant. Nevertheless, appropriate level of organic load is suggested to be considered for utilization of bubbling ozone, since as noted during experiments, reduction of MB concentration also exhibited to impair the chemical consumption of gaseous ozone (or effective use of ozone energy) that is responsible for global oxidative disruption of contaminants (namely the MB molecules and reductive intermediates for this study).

Supplementary material

The supplementary material for this paper is available online at http://dx.doi.10.1080/19443994.2015.1038592.

Acknowledgements

This work was financially supported by National Science and Technology Major Project (NO. 2012ZX07308-002) and National Natural Science Foundation of China (NO. 51478292).

References

[1] A.H. Konsowa, M.E. Ossman, Y. Chen, J.C. Crittenden, Decolorization of industrial wastewater by ozonation followed by adsorption on activated carbon, J. Hazard. Mater. 176 (2010) 181–185.
[2] K. Turhan, Z. Turgut, Treatment and degradability of direct dyes in textile wastewater by ozonation: A laboratory investigation, Desalin. Water Treat. 11 (2009) 184–191.
[3] R.F. Dantas, C. Sans, S. Esplugas, Ozonation of propranolol: Transformation, biodegradability, and toxicity assessment, J. Environ. Eng. 137 (2011) 754–759.
[4] M. Leili, G. Moussavi, K. Naddafi, Degradation and mineralization of furfural in aqueous solutions using heterogeneous catalytic ozonation, Desalin. Water Treat. 51 (2013) 6789–6797.
[5] J. Rivera-Utrilla, J. Méndez-Díaz, M. Sánchez-Polo, M.A. Ferro-García, I. Bautista-Toledo, Removal of the surfactant sodium dodecylbenzenesulphonate from water by simultaneous use of ozone and powdered activated carbon: Comparison with systems based on O_3 and O_3/H_2O_2, Water Res. 40 (2006) 1717–1725.
[6] F.J. Beltrán, J.F. García-Araya, I. Giráldez, Gallic acid water ozonation using activated carbon, Appl. Catal., B 63 (2006) 249–259.
[7] P.C.C. Faria, J.J.M. Órfão, M.F.R. Pereira, Catalytic ozonation of sulfonated aromatic compounds in the presence of activated carbon, Appl. Catal., B 83 (2008) 150–159.
[8] A.Y.C. Lin, S.C. Panchangam, C.Y. Chang, P.K.A. Hong, H.F. Hsueh, Removal of perfluorooctanoic acid and perfluorooctane sulfonate via ozonation under alkaline condition, J. Hazard. Mater. 243 (2012) 272–277.
[9] J. Staehelin, J. Hoigné, Decomposition of ozone in water: Rate of initiation by hydroxide ions and hydrogen peroxide, Environ. Sci. Technol. 16 (1982) 676–681.
[10] J.H.J. Kluytmans, B.G.M. van Wachem, B.F.M. Kuster, J.C. Schouten, Mass transfer in sparged and stirred reactors: Influence of carbon particles and electrolyte, Chem. Eng. Sci. 58 (2003) 4719–4728.
[11] A.H. Konsowa, Decolorization of wastewater containing direct dye by ozonation in a batch bubble column reactor, Desalination 158 (2003) 233–240.
[12] O.S.G.P. Soares, J.J.M. Órfão, D. Portela, A. Vieira, M.F.R. Pereira, Ozonation of textile effluents and dye solutions under continuous operation: Influence of operating parameters, J. Hazard. Mater. 137 (2006) 1664–1673.
[13] K. Turhan, Z. Turgut, Decolorization of direct dye in textile wastewater by ozonization in a semi-batch bubble column reactor, Desalination 242 (2009) 256–263.
[14] A.M.M. Vargas, A.L. Cazetta, M.H. Kunita, T.L. Silva, V.C. Almeida, Adsorption of methylene blue on activated carbon produced from flamboyant pods (Delonix regia): Study of adsorption isotherms and kinetic models, Chem. Eng. J. 168 (2011) 722–730.
[15] A. Petzer, B.H. Harvey, G. Wegener, J.P. Petzer, Azure B, a metabolite of methylene blue, is a high-potency, reversible inhibitor of monoamine oxidase, Toxicol. Appl. Pharmacol. 258 (2012) 403–409.
[16] R. Krishna, J. Ellenberger, S.T. Sie, Reactor development for conversion of natural gas to liquid fuels: A scale-up strategy relying on hydrodynamic analogies, Chem. Eng. Sci. 51 (1996) 2041–2050.
[17] T. Maezono, M. Tokumura, M. Sekine, Y. Kawase, Hydroxyl radical concentration profile in photo-Fenton oxidation process: Generation and consumption of hydroxyl radicals during the discoloration of azo-dye Orange II, Chemosphere 82 (2011) 1422–1430.
[18] M.L. Wilde, S. Montipó, A.F. Martins, Degradation of β-blockers in hospital wastewater by means of ozonation and Fe^{2+}/ozonation, Water Res. 48 (2014) 280–295.
[19] R.E. Bűhler, J. Staehelin, J. Hoigne, Ozone decomposition in water studied by pulse radiolysis. 1. HO_2/O_2- and HO_3/O_3- as intermediates, J. Phys. Chem. 88 (1984) 2560–2564.

[20] C.C.D. Yao, W.R. Haag, Rate constants for direct reactions of ozone with several drinking water contaminants, Water Res. 25 (1991) 761–773.
[21] W.H. Glaze, J.W. Kang, Advanced oxidation processes. Description of a kinetic model for the oxidation of hazardous materials in aqueous media with ozone and hydrogen peroxide in a semibatch reactor, Ind. Eng. Chem. Res. 28 (1989) 1573–1580.
[22] L.W. Lackey, R.O. Mines Jr., P.T. Mccreanor, Ozonation of acid yellow 17 dye in a semi-batch bubble column, J. Hazard. Mater. 138 (2006) 357–362.